Unconventional thermoelectric transport in tilted Weyl semimetals

Thorvald M. Ballestad,[1] Alberto Cortijo,[2] María A. H. Vozmediano,[3] and Alireza Qaiumzadeh[1]
[1]*Center for Quantum Spintronics, Department of Physics, Norwegian University of Science and Technology, Trondheim, Norway*
[2]*Departamento de Física de la Materia Condensada, Universidad Autónoma de Madrid, Madrid E-28049, Spain*
[3]*Instituto de Ciencia de Materiales de Madrid, CSIC, Cantoblanco, E-28049 Madrid, Spain*

(Received 28 September 2022; accepted 6 January 2023; published 13 January 2023)

We analyze the effect of the tilt on the transverse thermoelectric coefficient of Weyl semimetals in the *conformal* limit, i.e., zero temperature and zero chemical potential. Using the Kubo formalism, we find a nonmonotonic behavior of the thermoelectric conductivity as a function of the tilt perpendicular to the magnetic field, and a linear behavior when the tilt is aligned to the magnetic field. An "axial Nernst" current (chiral currents counter propagating perpendicularly to the magnetic field and the temperature gradient) is generated in inversion symmetric Weyl materials when the tilt vector has a projection in the direction of the magnetic field. This analysis will help in the design and interpretation of thermoelectric transport experiments in recently discovered topological quantum materials.

DOI: 10.1103/PhysRevB.107.014410

I. INTRODUCTION

Emergent low-energy massless quasiparticles in three-dimensional (3D) Dirac and Weyl semimetals (WSMs) provide a testbed for investigation of interesting phenomena beyond standard relativistic quantum field theory (QFT) and Landau Fermi liquid paradigm [1–3]. As opposed to the case in relativistic QFT, material models are not Lorentz invariant. In addition to the fact that massless Weyl quasiparticles move at the Fermi velocity—a hundred times smaller than the speed of light—other Lorentz breaking terms may appear in the low energy description of Dirac materials [4]. One generic feature of the dispersion relation in most 3D Dirac and WSMs not studied in QFT is the tilt of the cones [5]. According to its value, topological quantum semimetals are classified into type-I, having pointlike Fermi surface with vanishing density of states, and type-II WSMs with overtilted cones that have a hyperbolic Fermi surface with finite density of states at the Fermi level [1,6,7]. In some systems the tilting angle of Weyl cones and the topological Lifshitz phase transition [8] between type-I and type-II Weyl phases can be controlled by external perturbations [9,10].

One of the most interesting aspects of the physics of massless Dirac fermions in QFT is related to quantum anomalies [11]. They occur when a symmetry of a classical field theory action does not survive quantization [12–15]. The best-known quantum anomaly is the chiral anomaly associated to the nonconservation of the independent number of left- and right-handed Weyl fermions in a 3D massless Weyl system [12,13]. First identified in QFT as responsible for the fast decay of the neutral pion into two photons [16,17], is living a new bloom after its experimental realization in the modern condensed matter systems [18] where it gives rise to exotic thermo- and magnetoelectric transport phenomena [19–25].

A lesser-known quantum anomaly in condensed matter physics is the scale or conformal anomaly associated the quantum breakdown of scale invariance. The conservation of the corresponding Noether current (dilatation current) implies the traceless of the energy-momentum tensor [13–15], a condition that is violated after quantization in some anomalous QFTs. In the gravity context, it was recently shown that the scale anomaly leads to a new electromagnetic transport effect in the presence of an inhomogeneous gravitational background, the scale magnetic effect [26]. More recently, using the Luttinger theory of thermal transport [27], the scale magnetic effect was translated into an unconventional thermoelectric transport coefficient in 3D untilted Dirac and WSMs [28–30]. The very concrete prediction in Ref. [28] of the thermoelectric coefficient dependence on the magnetic field and temperature $\sim B/T$ is now being explored experimentally by several groups. For these delicate experiments, done as closed as possible to the conformal limit $T = 0$ and zero chemical potential, it is crucial to keep control of all the variables. The tilt is an important factor present in almost all real Dirac materials that does not break the scale invariance.

In this paper, we analyze the effect of the tilt in the previous context and develop a theory to investigate new unconventional thermomagnetoelectric effects in type-I Dirac and WSMs. We show that a tilt-dependent transverse current is induced by a temperature gradient in the presence of a perpendicular magnetic field. In tilted Dirac materials with full inversion symmetry, the tilt component parallel to the magnetic field gives rise to a novel axial (valley) current. Since the tilt is a generic feature of the topological semi-metals, this study will be useful in the design and analysis of experiments related to the thermoelectric transport at very low temperatures and electron densities.

II. THE MODEL

We consider an undoped topological WSM with and without inversion symmetry. Within the continuum model, a

tilted cone with chirality $s = \pm$ is described by the Hamiltonian [31],

$$\mathcal{H}_s = s v_F \sigma^i p_i + v_F t_s^i p_i I_2, \tag{1}$$

where v_F is the isotropic Fermi velocity, σ^i, $i = 1, 2, 3$ are the Pauli matrices, $\boldsymbol{p}$ is the momentum operator, and $\boldsymbol{t}^s$ is the tilt vector. The eigen energies of the Hamiltonian are

$$E_{\lambda s} = \lambda v_F |\boldsymbol{p}| + v_F t_s^i p_i, \tag{2}$$

where $\lambda = \pm$ refers to the conduction and valence bands, and we have set the reduced Planck constant $\hbar = 1$.

For the inversion symmetric, case we have $\boldsymbol{t}_s = s\boldsymbol{t}$, while for the broken inversion symmetry case, we will fix $\boldsymbol{t}_s = \boldsymbol{t}$. The transition from type I to type II WSMs occurs when $|t| > 1$ [32]. We will consider only type I tilted WSMs because the type II have an extended Fermi surface and cannot be modeled with the linear dispersion relation properly. Moreover, the finite density of states at the Fermi level introduces a dimension-full parameter in the model that breaks the scale invariance explicitly. We will investigate the type II WSMs elsewhere.

In four-dimensional combined space-time notation, the fermionic Lagrangian density is given by [2]

$$\mathcal{L}_{\mathrm{F}} = i\bar{\psi}\left[\gamma^0(\partial_0 - t^i\partial_i) + v_F\sum_{j=1}^{3}\gamma^j\partial_j\right]\psi, \tag{3}$$

where ψ is the fermionic field and γ^μ are the standard contravariant γ matrices [33].

Since the tilt vector coupling is dimensionless, the classical action remains scale invariant and the corresponding *canonical* energy-momentum tensor [34],

$$\mathcal{T}_s^{\mu\nu} = \tfrac{1}{2}(\Psi_s^\dagger\gamma_s^\mu\partial^\nu\Psi_s + \gamma_s^\nu\Psi_s^\dagger\partial^\mu\Psi_s - \eta^{\mu\nu}\mathcal{L}_s), \tag{4}$$

is traceless $(\mathcal{T}_s)_\mu^\mu = 0$. We consider a flat space Minkowski metric $\eta^{\mu\nu} = \mathrm{diag}(+1, -1, -1, -1)$. In Ref. [28] it was shown that, in the untilted case, the conformal anomaly in the presence of electric and magnetic fields, together with the Luttinger effective gravitational field theory of thermal transport, gives rise to an unconventional contribution to the thermoelectric transport coefficient. The formalism followed in Ref. [28] was explicitly Lorentz covariant. Since the tilt violates rotational invariance, we cannot follow this approach and we will compute the expected unconventional contribution with a Kubo formalism akin to that used in Ref. [29].

III. THE LUTTINGER APPROACH TO THE THERMOELECTRIC TRANSPORT COEFFICIENT

We will compute the thermoelectric transport coefficient in the presence of an applied magnetic field within a Kubo formula as devised by Luttinger in Ref. [27].

We chose the magnetic field to point along the z direction, $\boldsymbol{B} = B\hat{\boldsymbol{z}}$ and include it in the Hamiltonian (1) by the minimal coupling $\boldsymbol{p} \to \boldsymbol{p} + e\boldsymbol{A}$ where $e = |e|$ is the electron charge and $\boldsymbol{A} = -By\hat{\boldsymbol{x}}$ is the vector potential in the Landau gauge. For each chiral Weyl spinor, the Hamiltonian in the presence of the magnetic field reads

$$\mathcal{H}_s = s v_F \sigma^i (p_i + A_i) + v_F t_s^i p_i I_2. \tag{5}$$

We first assume that the tilt vector has a projected component along both the magnetic field $\boldsymbol{t}_s = t_s^z\hat{\boldsymbol{z}}$ and perpendicular to it $\boldsymbol{t}_s = t_s^x\hat{\boldsymbol{x}}$, and find the eigensystem of the Hamiltonian. Then, we investigate the effect of each component on the unconventional quantum transport in tilted undoped Weyl semimetals, separately.

To find the unconventional transverse thermoelectric response of undoped tilted WSMs in the presence of a temperature gradient, we use the Luttinger approach [27,35,36]. We introduce a gravitational scalar potential field ψ that couples to the energy density $\mathcal{T}^{00}$, into our electronic Hamiltonian as a perturbation $\mathcal{H}_L = \int d\boldsymbol{r}\psi\mathcal{T}^{00}$. The gradient of the gravitational field and temperature gradient ∇T are related by $\nabla\psi + \nabla T/T = 0$. Within the Kubo linear response formalism, the response of the system to the gradient of gravitational field can be found by applying the conservation of the energy–momentum tensor: $\partial_\mu T^{\mu 0} = \partial_t T^{00}/v_F + \partial_i T^{i0} = 0$. Within this formalism, the transverse thermoelectric susceptibility χ_s^{ij} of tilted Weyl quasiparticles, defined by

$$J_s^i = \chi_s^{ij}(-\partial_j T/T), \tag{6}$$

is given by the following retarded response function [29]:

$$\chi_s^{ij}(\omega, \boldsymbol{q}) = \frac{-iv_F}{\mathcal{V}}\int dt e^{i\omega t}\int_{-\infty}^{0} dt'\Theta(t) \times \langle[J_s^i(t, \boldsymbol{q}), \mathcal{T}^{j0}(t', -\boldsymbol{q})]\rangle, \tag{7}$$

where $\mathcal{V}$ is the system volume and Θ is the Heaviside step function. The details of the computation are depicted in the Appendix.

With all the previous ingredients (see the Appendix), we find the static and long-wavelength unconventional transverse response function of an undoped tilted WSM in the limit $T \to 0$ to be

$$\lim_{\omega\to 0}\lim_{\boldsymbol{q}\to 0}\chi_s^{xy} = \gamma_N(\boldsymbol{t}_s)\frac{e^2 v_F B}{2\hbar(2\pi)^2}, \tag{8}$$

where γ_N is a normalization factor that depends on the number of LLs N that are taken into account in the evaluation of the response function, and more importantly, on the tilting vector $\boldsymbol{t}^s$. This equation is our main result.

IV. THE INFLUENCE OF THE TILT ON THE THERMOELECTRIC COEFFICIENT

In general, we can decompose the normalization factor γ_N in Eq. (8) into an even and an odd function of the tilting parameter as $\gamma_N^{\mathrm{even(odd)}}(\boldsymbol{t}_s) = [\gamma_N(\boldsymbol{t}_s) \pm \gamma_N(-\boldsymbol{t}_s)]/2$. In the following, we will compute the normalization factor γ_N for type-I WSMs in different tilting geometries.

For the sake of completeness, we first look at the untilted case, first introduced in by Chernodub *et al.* [28] and Arjona *et al.* [29]. We have simplified their result and found an

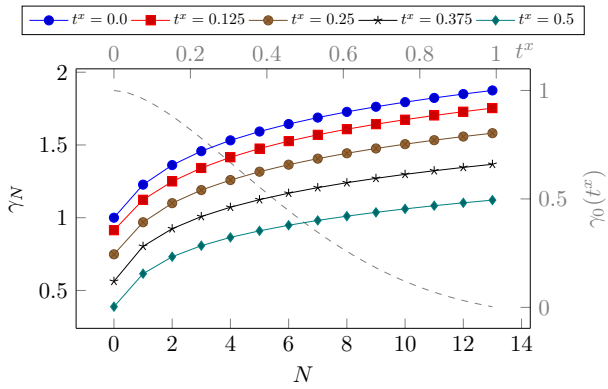

FIG. 1. The normalization factor γ_N, see Eqs. (8) and (9), as a function of the LLs cutoff N (solid lines) for various values of the tilt parameter perpendicular to the magnetic field direction $\boldsymbol{t} = t_s^x \hat{\boldsymbol{x}}$. The plot also present the tilt-dependence of the normalization factor for lowest LLs cutoff $N = 0$ (dashed gray line).

analytical expression for $\gamma_N(\boldsymbol{t}^s = 0)$ with $N \geqslant 0$, as

$$\gamma_N - \gamma_{N-1} = \gamma_{N=0} + 2N\{1 - (1+N)\log(1+N^{-1})\},$$

where $\gamma_{N=0} = 1$ and by definition $\gamma_{N=-1} = 0$.

A. Tilt perpendicular to the applied magnetic field

When the tilt vector of the Weyl cone is perpendicular to the applied magnetic field, $\boldsymbol{t} \perp \boldsymbol{B}$, we find

$$\gamma_N(t_s^x) = -4\hbar v_F \beta^3 \sum_{m>0,n\leqslant 0}^{N} \int dk_z e^{-P^2} \times \frac{\alpha_{k_z ms}^2 \left(\Xi_{m,n,s}^{(1)}\right)^2 (E_{k_z ms} + E_{k_z ns})}{\left(\alpha_{k_z ms}^2 + 1\right)\left(\alpha_{k_z ns}^2 + 1\right)(E_{k_z ms} - E_{k_z ns})^2}, \quad (9)$$

where the integration limit is $(-\infty, \infty)$, except for $n = 0$, where it is $[0, \infty)$. In this case, the normalization factor is an even function of tilting, and thus independent of the chirality s. The response was solved numerically and the result is shown in Fig. 1. As the tilt increases, the $\gamma_{N=0}$ decreases monotonically. In Fig. 1, we present the normalization factor γ_N as a function of the LL cutoff N, for various tilt parameters t^x.

The sum over LLs is bounded by considering all transitions between LLs below some cutoff level N. In the untilted case, in the deep quantum limit where only the lowest LL is filled, one may only take into account $0 \to \pm 1$ transitions. However, in the case of perpendicular tilt, where the dipolar selection rule $|m| = |n| + 1$ is not valid anymore, it might be reasonable to consider higher transitions $0 \to n$ with $|n| \leqslant N$. Considering these transitions, we find a qualitatively different response. The response of the system shows a nonmonotonic behavior as a function of tilting parameter; see Fig. 2. It has a maximum at a critical titling value and then decreases and vanishes as $|t^x| \to 1$. We will discuss this emergent feature in Sec. V.

B. Tilt parallel to the magnetic field

When the tilt vector is parallel to the magnetic field, it can be shown that the response of the tilt term in the Hamiltonian is algebraically added to the untilted response

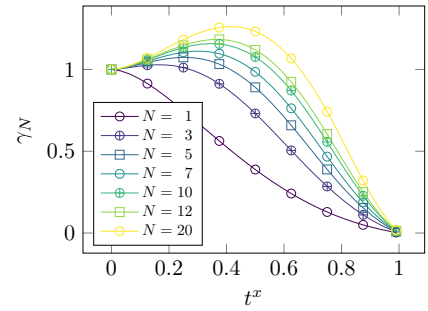

FIG. 2. The normalization factor γ_N, Eqs. (8) and (9), as a function of the tilt parameter perpendicular to the magnetic field direction $\boldsymbol{t} = t_s^x \hat{\boldsymbol{x}}$, for various LLs cutoff N.

function, $\gamma_N(t_s^z) = \gamma_N(\boldsymbol{t}^s = 0) + \delta\gamma_N(t_s^z)$, where

$$\delta\gamma_N(t_s^z) = -8t_s^z \hbar^2 v_F^2 \sum_{i=0}^{N} \int_{-\infty}^{k_z^c} dk_z k_z \frac{\alpha_{k_z ms}^2}{\left[\left(\alpha_{k_z ms}^2 + 1\right)\left(\alpha_{k_z ns}^2 + 1\right)\right]} \times \frac{n_{k_z ms} - n_{k_z ns}}{(E_{k_z ms} - E_{k_z ns})^2}\Bigg|_{\substack{m=i+1 \\ n=-i}}, \quad (10)$$

with $n_{k_z ms}$ is the equilibrium Fermi-Dirac distribution function. Since we are using a linearized model Hamiltonian to describe the low-energy Weyl quasiparticles, this contribution is logarithmically divergent, so we introduce an ultraviolet wave number cutoff k_z^c to get,

$$\frac{\delta\gamma_N - \delta\gamma_{N-1}}{2t_s^z} = \Lambda(\sqrt{\Lambda^2 + N} - \sqrt{\Lambda^2 + N + 1}) + (N+1)\tanh^{-1}\left[\frac{\Lambda}{\sqrt{\Lambda^2 + N + 1}}\right] - N\tanh^{-1}\left[\frac{\Lambda}{\sqrt{\Lambda^2 + N}}\right], \quad (11)$$

for $N \geqslant 0$, where $\Lambda = l_B k_z^c/\sqrt{2}$ is the dimensionless wave number cutoff and by definition $\delta\gamma_{-1} = 0$. We estimate the ultraviolet cutoff as $k_z^c \approx 1/a$, where a is the lattice constant of a Weyl or Dirac semimetal.

Figure 3 shows the contribution to the total normalization factor of a finite tilt parameter parallel to the magnetic field, as a function of the ultraviolet wave number cutoff and for various LLs cutoff.

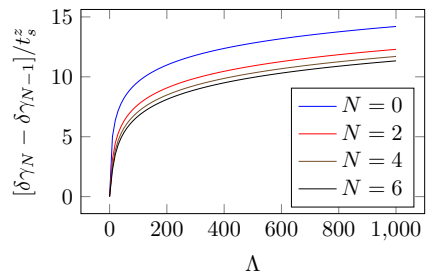

FIG. 3. The normalization factor γ_N, Eqs. (8) and (11), as a function of the dimensionless wave number cutoff for various LLs cutoff N, when the tilt parameter $\boldsymbol{t} = t_s^z \hat{\boldsymbol{z}}$ is parallel to the magnetic field direction.

This term is odd in the tilt vector, and thus in the inversion symmetric case, its contribution to the total normalization factor of the two Weyl cones is zero, and thus the tilting has no contribution to the total charge current J_c^i. However, this term will have a contribution to a valley (or axial) current $J_A^i \equiv J_+^i - J_-^i$. Therefore, we will find an "axial Nernst" current perpendicular to an applied magnetic field and to a gradient of temperature, in the conformal limit (zero temperature and zero chemical potential) in inversion symmetric tilted WSMs.

V. DISCUSSION

In this section we will discuss the salient features arising from Eq. (9). For any direction of the tilt vector $\boldsymbol{t}_s$, the function $\gamma_N(\boldsymbol{t}_s)$ is not bounded when including more Landau level transitions in the computation of Eq. (9). This response is also (logarithmically) divergent as the cutoff Λ grows, as we can see in Fig. 3 for the particular case $\boldsymbol{t}_s = t_s^z \hat{\boldsymbol{z}}$, in contrast to, for instance, what happens with the electric conductivity. This has been discussed previously in untilted case [29]. The physical origin of this divergence is traced to the larger engineering dimension of the energy-momentum operator $\mathcal{T}^{0j}$ compared with the current operator J^i, as it can be readily seen in Eq. (4). Also, as we are working in the limit of zero temperature and the Fermi level crossing the nodal point, transport properties are dominated by interband transitions, so we expect to obtain more reliable results when incorporating higher LL transitions, controlled by the cutoff parameter N. What is more surprising is the presence of a maximum in $\gamma_N(\boldsymbol{t}_s)$, when the tilt vector is perpendicular to $\mathbf{B}$ (in our case, $\boldsymbol{t}_s = t^x \hat{\boldsymbol{x}}$), as it can be appreciated in Fig. 2. In absence of tilt, $\gamma_N(\boldsymbol{t}_s = 0) = 1$, that agrees with previous results based on the conformal anomaly [28]. However, as discussed in the Introduction, the presence of a tilt vector $\boldsymbol{t}_s$, being a velocity, does not spoil scale invariance at the classical level as it does not introduce any scale in the problem, so a particular preferred value of $\boldsymbol{t}_s$ should not be expected. Also, the presence of a maximum in response functions often implies the competition of several effects. Besides, this maximum does not appear when $\boldsymbol{t}_s$ is parallel to the magnetic field $\mathbf{B}$. In fact, a linearly increasing γ_N is expected (at least at small values of $\boldsymbol{t}_s$) as the current operator J_s^i possesses a linear contribution with $\boldsymbol{t}_s$, as it can be seen in Eq. (A3), for any tilt direction, and this dependence qualitatively explains why γ_N grows when $\boldsymbol{t}_s = t_i^x \hat{\boldsymbol{x}}$ in Fig. 2. To understand the change of monotony in $\gamma_N(t_i^x \hat{\boldsymbol{x}})$ it is instructive to interpret the presence of the tilt vector in the Weyl Hamiltonian in terms of an emergent Lorentz symmetry [32,37–39]. WSMs possess an emergent symmetry in form of Lorentz invariance, where the role of the speed of light is played by the Fermi velocity v_F, as can be readily seen in the Lagrangian (3). The presence of a tilt vector breaks this emergent Lorentz invariance selecting a preferred reference frame (lab frame) with velocity $\boldsymbol{t}_s$. Although this symmetry is broken by the tilt, we can still Lorentz transform the Hamiltonian to get rid of the tilt (tilt frame), compute the spectrum as in absence of the tilt and get back to the laboratory frame. The price to pay is that energies, momenta, and other vectors get modified (rescaled) by the presence of the squeezing factor $\beta = \sqrt{1 - (\boldsymbol{t}_s)^2}$, which is the rapidity in the language of special relativity, and it is permissible when

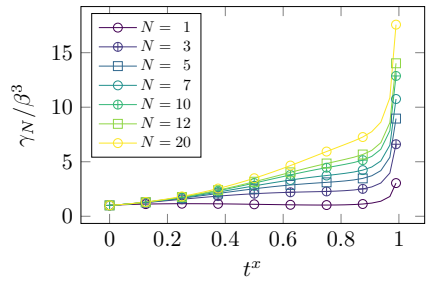

FIG. 4. Same situation as Fig. 2 but with the normalization factor divided by β^3: γ_N/β^3 as a function of the value of the tilt perpendicular to the magnetic field $\boldsymbol{t}_s = t_s^x \hat{\boldsymbol{x}}$.

$\boldsymbol{t}_s < 1$. We also know that in this regime, the effective magnetic field $\mathbf{B}$ acting in the tilt frame is reduced (squeezed) with respect to the magnetic field in the laboratory frame, $\mathbf{B}' = \beta^3 \mathbf{B}_{\text{lab}}$ [38]. This squeezing factor β^3 appears explicitly in Eq. (9) accompanying the magnetic field $\mathbf{B}(= \mathbf{B}_{\text{lab}})$. We have plotted in Fig. 4 the normalization factor γ_N divided by β^3. Now we observe that the rescaled normalization factor γ_N/β^3 monotonically grows with the tilt parameter, linearly for small tilt, due to the presence of the tilt term in the current operator J_s^i, and it diverges (within our numerical accuracy) when t^x approaches to 1. This divergence appears in other transport properties of tilted WSMs [32,39]. Then, the presence of a maximum in γ_N for tilts perpendicular to the magnetic field is a competition from the fact that there is a piece of the electric current that is enhanced due to the tilt at low tilts (and eventually diverges when $t^x \to 1$), and the squeezing factor that modifies the effective magnetic field that decreases.

When the tilt vector points along the magnetic field, such squeezing of the effective magnetic field does not occur, so the only term depending of the tilt vector is the one present in the current operator and we expect a monotonously increasing behavior (linear at low t_s^z) of γ_N. This behavior is plotted in Fig. 5. Both effects are kinematic effects and do not spoil the scale anomaly responsible of the universal value at $\boldsymbol{t}_s = 0$.

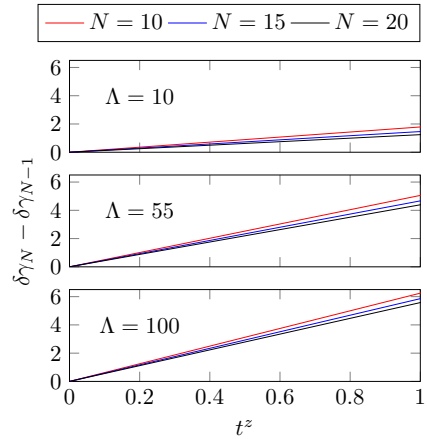

FIG. 5. Linear behavior of the normalization factor as a function of the tilt parameter parallel to the magnetic field, Eq. (11), for various values of the wave number cutoff Λ and LL truncation N.

To finish this section, we would like to comment on what we can expect for the transport coefficient χ^{xy} when the tilt, being perpendicular to the magnetic field, points along the direction $\hat{\boldsymbol{y}}$ (the direction of ∇T) instead of pointing along $\hat{\boldsymbol{x}}$ (the direction of the computed current), as discussed in the previous section. According to the point of view adopted here, under the condition of the tilt vector $\boldsymbol{t}$ to be perpendicular to $\mathbf{B}$, a Lorentz transformation made to the tilted system is formally equivalent to study the system with no tilt but in the presence of effective magnetic and electric fields, $\mathbf{B}'$ and $\mathbf{E}' \sim \boldsymbol{t}$, the latter pointing along $\hat{\boldsymbol{y}}$. This implies the presence of a drift velocity that points perpendicularly to both $\mathbf{B}'$ and $\mathbf{E}' \sim \boldsymbol{t}$, that is, $\boldsymbol{v}_d$ pointing along $\hat{\boldsymbol{x}}$ that also scales with t^y as it does $\mathbf{E}'$. This drift velocity would generate a component of the current J^x that scales with t^y that is not contained explicitly in the operator J^x in Eq. (A3), as, remember, the tilt now points along $\hat{\boldsymbol{y}}$. Also, as $\boldsymbol{t}$ is still perpendicular to $\mathbf{B}$, there will be a squeezing of the magnetic field in the transformed reference frame $\mathbf{B}'$.

Then, we expect a similar qualitative behavior to the case when $\boldsymbol{t} = t\hat{\boldsymbol{x}}$ shown in Fig. 2 and discussed at the beginning of this section. The coefficient of the thermoelectric conductivity will grow with t for small values of t^y due to the presence of the drift velocity along $\hat{\boldsymbol{x}}$ that scales linearly with t^y, and, for larger values of t^y the squeezing of the effective magnetic field will dominate and make it decrease.

VI. CONCLUSION

We have investigated the effect of Weyl cone tilting in Dirac and WSMs on the novel thermoelectric response based on the conformal anomaly, proposed in Refs. [28,29]. We show that the thermoelectric response function of undoped WSMs is sensitive to the tilt vector parameter and to its relative angle with respect to the external magnetic field. This dependence of the response function to the tilt parameter and magnetic field may be an important signature in experimental measurements to disentangle different thermoelectric responses in their signals and extract the conformal anomaly contribution. In particular, when the tilt vector is parallel to the magnetic field, the scale-anomaly argument still produces a lower bound to the corresponding Nernst coefficient, but this is not the case when the tilt vector is perpendicular to $\mathbf{B}$. we found an "axial thermoelectric effect," i.e., the generation of an axial current perpendicular to an applied magnetic field and to a gradient of temperature, originated in the conformal anomaly in tilted WSMs with inversion symmetry when the tilt vector has is a projection in the direction of the magnetic field. It is interesting to mention that an "axial" anomalous Nernst coefficient for tilted WSMs in the absence of external magnetic fields have been found to be proportional to the tilt vector, as the nodal separation is the vector playing the role of "axial" magnetic field [40]. The axial current as a response of the magnetic field, found in the present paper, is thus the reciprocal transport coefficient predicted in Ref. [40].

The effects of the tilt of the cones on the transport properties of other Dirac materials in two and three spacial dimensions has been analyzed previously in the literature [41–45]. The special feature of the present work lies on its connection to the conformal anomaly, which only occurs in (1+1) and (3+1) space-time dimensions.

ACKNOWLEDGMENTS

This project has been supported by the Norwegian Financial Mechanism Project No. 2019/34/H/ST3/00515, "2Dtronics"; and partially by the Research Council of Norway through its Centres of Excellence funding scheme, Project No. 262633, "QuSpin." This work is also part of Project No. PGC2018-099199-B-I00 funded by Grant No. MCIN/AEI/10.13039/501100011033 and by ERDF A way of making Europe. A.C. acknowledges financial support from the Ministerio de Ciencia e Innovación through Grant No. PID2021-127240NB-I00 and the Ramón y Cajal program through Grant No. RYC2018- 023938-I

APPENDIX: KUBO FORMULA FOR THE THERMOELECTRIC TRANSPORT COEFFICIENT

In what follows, we will set the basic ingredients to compute the thermoelectric transport coefficient in the presence of an applied magnetic field within a Kubo formula. The Landau levels (LLs) of the tilted WSMs have been computed in Refs. [32,38]. As it is known, the 3D LLs are dispersing in the direction of the applied magnetic field. For the assumed geometry with the magnetic field pointing in the z direction, and using a generic plane wave ansatz $\phi(\boldsymbol{r}) = e^{ik_x x + ik_z z}\phi(y)$, the spectrum of Eq. (5) is given by

$$E_{k_z ms} = \begin{cases} t_s^z v_F k_z + \mathrm{sign}(m) v_F \beta \sqrt{2eB\beta|m| + k_z^2}, & m \neq 0, \\ t_s^z v_F k_z - s\beta v_F k_z; & m = 0, \end{cases} \tag{A1}$$

where β is a *squeezing factor* $\beta = \sqrt{1-(t_s^x)^2}$. In absence of the tilt vector, $\boldsymbol{t}_s = 0$ and $\beta = 1$, this LL spectrum reduces to the dispersion of the untilted case $E^0_{k_z ms}(B)$ [29]. The corresponding eigenstates are

$$\phi_m(y) = \frac{\beta^{1/2} e^{\sigma_x \theta_s/2} e^{-\chi_m^2/2}}{(L_x L_z)^{1/2}} \begin{pmatrix} a_{k_z ms} H_{|m|-1}(\chi_m) \\ b_{k_z ms} H_{|m|}(\chi_m) \end{pmatrix}, \tag{A2}$$

where $H_n(x)$ are the Hermite polynomials, $\theta_s = -s \tanh^{-1} t_x$, $l_B = \sqrt{1/(eB)}$ is the magnetic length, and $L_{x(z)}$ is the system size along the $x(z)$ direction. We also define

$$\chi_m = \beta^{1/2}(y/l_B - k_x l_B) + \tfrac{t_s^x l_B}{\beta^{1/2} v_F} E^0_{k_z ms}(\beta B),$$

$$a_{k_z ms} = \frac{\alpha_{k_z ms}(\beta/\pi)^{1/4}}{\sqrt{\left(\alpha^2_{k_z ms}+1\right) l_B 2^{|m|-1}(|m|-1)!}},$$

and

$$b_{k_z ms} = \frac{(\beta/\pi)^{1/4}}{\sqrt{\left(\alpha^2_{k_z ms}+1\right) l_B 2^{|m|}|m|!}},$$

with

$$\alpha_{k_z ms} = \frac{-(\beta|m|)^{1/2}}{\mathrm{sign}(m) s \sqrt{\beta|m| + l_B^2 k_z^2/2} - l_B k_z/\sqrt{2}}.$$

It is interesting to note that the LLs collapse when $|t_s^x| \geqslant 1$ [32,46,47] which is the condition for the transition from type

I to type II WSMs. This can be seen from the expression of β and θ_s. Since the distance between the LLs is reduced by a factor $\beta^{3/2}$, the separation between LLs vanishes in the limit of $|t_s^x| \to 1$ and $\beta \to 0$. On the contrary, there is no restriction on the value of the parallel tilt t_s^z. The energy levels are tilted by the parallel component of the tilt vector onto the magnetic field t_z, while the perpendicular component t_x squeezes the separation between the levels.

We will consider the charge current operator at each Weyl node,

$$J_s^i = sev_F\tilde{\sigma}_s^i, \tag{A3}$$

where we have defined modified Pauli matrices as $\tilde{\sigma}_s^i = \sigma^i + st_s^i\sigma^0$. We can define the total charge current as $J_c^i = J_+^i + J_-^i$ and charge-neutral valley current as $J_v^i = J_+^i - J_-^i$. Without loss of generality, in the following, we assume $\nabla T \parallel \hat{\boldsymbol{y}}$, and compute the transverse charge current $\boldsymbol{J}_s \parallel \hat{\boldsymbol{x}}$ in the presence of a magnetic field along the z direction.

In systems with broken time-reversal symmetry, the total current, computed within the linear response theory, is the sum of an observable transport current and a circulating orbital magnetization current that does not contribute to the observable current [36,48]. Since we are interested in the undoped case, the diamagnetic-like orbital magnetization is zero and the Kubo formalism only gives the observable charge current [48].

To investigate the unconventional transport arising from the scale anomaly, we should compute the static transverse response of the system at the long-wavelength limit. After some tedious but straightforward analytical calculations [49], we find the charge current density

$$J_s^x = sev_F\beta^2\sum_{\boldsymbol{kmn}} J^x_{\boldsymbol{kms};\boldsymbol{kns}}$$

and energy-momentum tensor

$$T_s^{y0} = \frac{is\beta}{2}\sum_{\boldsymbol{kmn}} T^{y0}_{\boldsymbol{kns},\boldsymbol{kms}}$$

expressed in terms of the corresponding matrix elements, that are given by

$$J^x_{\boldsymbol{kms};\boldsymbol{kns}} = \left[\alpha_{k_zms}\Xi^{(1)}_{m,n,s} + \alpha_{k_zns}\Xi^{(2)}_{m,n,s}\right]\Gamma_{\boldsymbol{kmns}}, \tag{A4}$$

$$T^{y0}_{\boldsymbol{kns},\boldsymbol{kms}} = \left[\alpha_{k_zms}\Xi^{(1)}_{m,n,s} - \alpha_{k_zns}\Xi^{(2)}_{m,n,s}\right]\Gamma_{\boldsymbol{kmns}} \times \left(E_{k_zms} + E_{k_zns}\right). \tag{A5}$$

In the above equations, we have defined

$$\Gamma_{\boldsymbol{kmns}} = \frac{\exp\left\{-\left[l_B^2(t^x)^2/4v_F^2\beta\right]\left[E^0_{k_zns}(\beta B) - E^0_{k_zms}(\beta B)\right]^2\right\}}{\sqrt{\left(\alpha^2_{k_zms}+1\right)\left(\alpha^2_{k_zns}+1\right)}},$$

and

$$\Xi^{(1)} = \begin{cases} \Xi[|n|,|m|,P], & |n| \geqslant |m|-1, \\ \Xi[|n| \leftrightarrow (|m|-1), P \to -P], & |n| \leqslant |m|-1, \end{cases}$$

$$\Xi^{(2)} = \begin{cases} \Xi[|n| \leftrightarrow |n-1|, |m| \leftrightarrow |m-1|], & |n|-1 \geqslant |m|, \\ \Xi[|n| \leftrightarrow |m|, P \to -P], & |n|-1 \leqslant |m|, \end{cases}$$

where $\Xi = \sqrt{\frac{2^{|n|}(|m|-1)!}{2^{|m|-1}|n|!}}\left(\frac{P}{\sqrt{2}}\right)^{|n|-|m|+1}L_{|m|-1}^{(|n|-|m|+1)}(P^2)$, with $L_n^{(\alpha)}(x)$ is the generalized Laguerre polynomial and $P = st^x l_B[E^0_{k_zns}(\beta B) - E^0_{k_zms}(\beta B)]/(v_F\sqrt{2\beta})$.

[1] B. Q. Lv, T. Qian, and H. Ding, Experimental perspective on three-dimensional topological semimetals, Rev. Mod. Phys. **93**, 025002 (2021).

[2] N. P. Armitage, E. J. Mele, and A. Vishwanath, Weyl and Dirac semimetals in three-dimensional solids, Rev. Mod. Phys. **90**, 015001 (2018).

[3] Z. Lu, P. Hollister, M. Ozerov, S. Moon, E. D. Bauer, F. Ronning, D. Smirnov, L. Ju, and B. J. Ramshaw, Weyl Fermion magneto-electrodynamics and ultralow field quantum limit in TaAs, Sci. Adv. **8**, eabj1076 (2022).

[4] V. A. Kostelecký, R. Lehnert, N. McGinnis, M. Schreck, and B. Seradjeh, Lorentz violation in Dirac and Weyl semimetals, Phys. Rev. Res. **4**, 023106 (2022).

[5] B. Jiang, J. Zhao, J. Qian, S. Zhang, X. B. Qiang, L. Wang, R. Bi, J. Fan, H.-Z. Lu, E. Liu, and X. Wu, Antisymmetric Seebeck Effect in a Tilted Weyl Semimetal, Phys. Rev. Lett. **129**, 056601 (2022).

[6] A. A. Soluyanov, D. Gresch, Z. Wang, Q. Wu, M. Troyer, X. Dai, and B. A. Bernevig, Type-II Weyl semimetals, Nature (London) **527**, 495 (2015).

[7] Y. Xu, F. Zhang, and C. Zhang, Structured Weyl Points in Spin-Orbit Coupled Fermionic Superfluids, Phys. Rev. Lett. **115**, 265304 (2015).

[8] G. E. Volovik, Topological Lifshitz transitions, Low Temp. Phys. **43**, 47 (2017).

[9] C.-K. Chan, Y.-T. Oh, J. H. Han, and P. A. Lee, Type-II Weyl cone transitions in driven semimetals, Phys. Rev. B **94**, 121106(R) (2016).

[10] H. F. Yang, L. X. Yang, Z. K. Liu, Y. Sun, C. Chen, H. Peng, M. Schmidt, D. Prabhakaran, B. A. Bernevig, C. Felser, B. H. Yan, and Y. L. Chen, Topological Lifshitz transitions and fermi arc manipulation in Weyl semimetal NbAs, Nat. Commun. **10**, 3478 (2019).

[11] R. A. Bertlmann, *Anomalies in Quantum Field Theory*, Oxford Science Publications No. 91 (Clarendon Press, Oxford /New York, 1996)

[12] G. E. Marsh, The chiral anomaly, Dirac and Weyl semimetals, and force-free magnetic fields, Can. J. Phys. **95**, 711 (2017).

[13] A. Zee, *Quantum Field Theory in a Nutshell*, 2nd ed. (Princeton University Press, Princeton, NJ, 2010).

[14] E. Fradkin, *Quantum Field Theory: An Integrated Approach*, 1st ed. (Princeton University Press, Princeton, NJ, 2021).

[15] M. Shifman, *Advanced Topics in Quantum Field Theory*, 2nd ed. (Cambridge University Press, Cambridge, UK, 2022).

[16] S. L. Adler, Axial-vector vertex in spinor electrodynamics, Phys. Rev. **177**, 2426 (1969).
[17] J. S. Bell and R. Jackiw, A PCAC puzzle: $\pi^0 \to \gamma\gamma$ in the σ-model, Il Nuovo Cimento A (1965–1970) **60**, 47 (1969).
[18] N. P. Ong and S. Liang, Experimental signatures of the chiral anomaly in Dirac-Weyl semimetals, Nat. Rev. Phys. **3**, 394 (2021).
[19] A. A. Burkov, Chiral anomaly and transport in Weyl metals, J. Phys.: Condens. Matter **27**, 113201 (2015).
[20] T. Wehling, A. Black-Schaffer, and A. Balatsky, Dirac materials, Adv. Phys. **63**, 1 (2014).
[21] A. A. Burkov, Topological semimetals, Nat. Mater. **15**, 1145 (2016).
[22] E. V. Gorbar, V. A. Miransky, and I. A. Shovkovy, Chiral anomaly, dimensional reduction, and magnetoresistivity of Weyl and Dirac semimetals, Phys. Rev. B **89**, 085126 (2014).
[23] K. Das and A. Agarwal, Thermal and gravitational chiral anomaly induced magneto-transport in Weyl semimetals, Phys. Rev. Research **2**, 013088 (2020).
[24] K. Das, S. K. Singh, and A. Agarwal, Chiral anomalies induced transport in Weyl metals in quantizing magnetic field, Phys. Rev. Research **2**, 033511 (2020).
[25] K. Das and A. Agarwal, Berry curvature induced thermopower in type-I and type-II Weyl semimetals, Phys. Rev. B **100**, 085406 (2019).
[26] M. N. Chernodub, Anomalous Transport Due to the Conformal Anomaly, Phys. Rev. Lett. **117**, 141601 (2016).
[27] J. M. Luttinger, Theory of thermal transport coefficients, Phys. Rev. **135**, A1505 (1964).
[28] M. N. Chernodub, A. Cortijo, and M. A. H. Vozmediano, Generation of a Nernst Current from the Conformal Anomaly in Dirac and Weyl Semimetals, Phys. Rev. Lett. **120**, 206601 (2018).
[29] V. Arjona, M. N. Chernodub, and M. A. H. Vozmediano, Fingerprints of the conformal anomaly on the thermoelectric transport in Dirac and Weyl semimetals: Result from a Kubo formula, Phys. Rev. B **99**, 235123 (2019).
[30] V. Arjona Romano, Novel thermoelectric and elastic responses in Dirac matter, Ph.D. thesis, Autonomous University of Madrid, Madrid, Spain, 2019.
[31] M. O. Goerbig, J.-N. Fuchs, G. Montambaux, and F. Piéchon, Tilted anisotropic Dirac cones in quinoid-type graphene and α-(BEDT-TTF)$_2$i$_3$, Phys. Rev. B **78**, 045415 (2008).
[32] S. Tchoumakov, M. Civelli, and M. O. Goerbig, Magnetic-Field-Induced Relativistic Properties in Type-I and Type-II Weyl Semimetals, Phys. Rev. Lett. **117**, 086402 (2016).
[33] M. E. Peskin and D. V. Schroeder, *An Introduction to Quantum Field Theory* (Addison-Wesley, Reading, MA, 1995).
[34] M. Forger and H. Römer, Currents and the energy-momentum tensor in classical field theory: A fresh look at an old problem, Ann. Phys. **309**, 306 (2004).
[35] G. Tatara, Thermal Vector Potential Theory of Transport Induced by a Temperature Gradient, Phys. Rev. Lett. **114**, 196601 (2015).
[36] M. N. Chernodub, Y. Ferreiros, A. G. Grushin, K. Landsteiner, and M. A. Vozmediano, Thermal transport, geometry, and anomalies, Phys. Rep. **977**, 1 (2022).
[37] M. Udagawa and E. J. Bergholtz, Field-Selective Anomaly and Chiral Mode Reversal in Type-II Weyl Materials, Phys. Rev. Lett. **117**, 086401 (2016).
[38] Z.-M. Yu, Y. Yao, and S. A. Yang, Predicted Unusual Magnetoresponse in Type-II Weyl Semimetals, Phys. Rev. Lett. **117**, 077202 (2016).
[39] S. Rostamzadeh, I. Adagideli, and M. O. Goerbig, Large enhancement of conductivity in Weyl semimetals with tilted cones: Pseudorelativity and linear response, Phys. Rev. B **100**, 075438 (2019).
[40] Y. Ferreiros, A. A. Zyuzin, and J. H. Bardarson, Anomalous Nernst and thermal hall effects in tilted Weyl semimetals, Phys. Rev. B **96**, 115202 (2017).
[41] A. Martín-Ruiz and A. Cortijo, Parity anomaly in the nonlinear response of nodal-line semimetals, Phys. Rev. B **98**, 155125 (2018).
[42] I. Mandal and K. Saha, Thermopower in an anisotropic two-dimensional Weyl semimetal, Phys. Rev. B **101**, 045101 (2020).
[43] M. Stålhammar, J. Larana-Aragon, J. Knolle, and E. J. Bergholtz, Magneto-optical conductivity in generic Weyl semimetals, Phys. Rev. B **102**, 235134 (2020).
[44] C. Wang, W.-H. Xu, C.-Y. Zhu, J.-N. Chen, Y.-L. Zhou, M.-X. Deng, H.-J. Duan, and R.-Q. Wang, Anomalous hall optical conductivity in tilted topological nodal-line semimetals, Phys. Rev. B **103**, 165104 (2021).
[45] S. Yadav, S. Sekh, and I. Mandal, Magneto-optical conductivity in the type-I and type-II phases of Weyl/multi-Weyl semimetals, arXiv:2207.03316 (2022).
[46] V. Lukose, R. Shankar, and G. Baskaran, Novel Electric Field Effects on Landau Levels in Graphene, Phys. Rev. Lett. **98**, 116802 (2007).
[47] V. Arjona, E. V. Castro, and M. A. H. Vozmediano, Collapse of Landau levels in Weyl semimetals, Phys. Rev. B **96**, 081110(R) (2017).
[48] E. C. I. van der Wurff and H. T. C. Stoof, Magnetovortical and thermoelectric transport in tilted Weyl metals, Phys. Rev. B **100**, 045114 (2019).
[49] T. M. Ballestad, Anomalous thermoelectric effect in tilted Dirac and Weyl Semimetals, Master's thesis, Norwegian University of Science and Technology (NTNU), Trondheim, Norway, 2022.